International Journal of Heat and Mass Transfer 51 (2008) 5918–5930

Contents lists available at ScienceDirect

International Journal of Heat and Mass Transfer

journal homepage: www.elsevier.com/locate/ijhmt

Transient coupled heat transfer in an anisotropic scattering composite slab with semitransparent surfaces

Hong-Liang Yi, Ming Xie, He-Ping Tan *

School of Energy Science and Engineering, Harbin Institute of Technology, 92 West Dazhi Street, Harbin 150001, PR China

ARTICLE INFO

Article history:
Received 24 December 2007
Received in revised form 9 April 2008
Available online 18 June 2008

Keywords:
Coupled heat transfer
Radiation
Composite
Radiative transfer coefficients
Anisotropic scattering
Total reflection

ABSTRACT

Transient heat transfer of coupled radiation and conduction inside a semitransparent composite slab of absorbing–emitting-anisotropic scattering medium is examined. The composite slab includes two layers with different physical properties. Surfaces and interface between two layers are supposed to be semitransparent and total reflection will occur there at the critical angle. Specular reflection is considered and reflectivities are determined by Fresnel's law and Snell's law. A fully implicit control-volume method is used to solve the transient energy equation and a ray-tracing/nodal-analyzing method is used to compute the radiative information. A criterion for total reflection is proposed for solving the problem of integral singularity at the critical angle. Effects of conduction–radiation parameter, scattering albedo and refractive index on coupled heat transfer are investigated. Results show that in a semitransparent medium with natural surfaces, there are two sorts of temperature peaks appearing at transient heat transfer: one is caused by external radiation heating and environmental convection cooling, still existing in steady state; the other is due to maximum of absorption of heat caused by inhomogeneous optical properties, only existing in transients of heat transfer.

1. Introduction

Coupled radiative and conductive heat transfer is the main mode of energy transfer in a semitransparent solid medium at elevated temperatures, in high temperature surroundings, with large incident radiation, or in vacuum circumstances with weak convection of low and moderate temperature. Some errors will be caused if only considering conduction or radiation. For a long time, considerable attention has been given to the problem for its many important applications, such as multilayer spaceborne optical windows, combustion fabrication device, the insulation properties of fibrous and ceramic materials.

A solution to coupled radiation–conduction involves two parts: the solution to the radiative transfer equation, and the solution to the energy equation. An evaluation of the former can adopt such methods as DOM (discrete ordinates method), DTM (discrete transfer method), flux method, RTNAM (ray-tracing/nodal-analyzing method), zone method, FVM (finite-volume method) and so on. The latter can be solved using FDM (finite difference method), FVM, FEM (finite element method), LBM (lattice Boltzmann Method) and meshless method.

Muresan et al. [1] solved the coupled conductive radiative heat transfer in a two-layer non-scattering slab with Fresnel interfaces subject to diffuse and obliquely collimated irradiation using a DOM for the solution to the radiative transfer problem and a FDM for the solution to the energy equation. In Ref. [1], adaptive directional quadratures were developed to overcome the difficulties usually encountered at the interfaces. Mishra et al. [2] examined transient conductive–radiative heat transfer in a 2-D rectangular enclosure filled with an optically absorbing, emitting and scattering medium using LBM for the solution to the energy equation and the collapsed dimension method for the radiative transfer equation, and analyzed the effects of the conduction–radiation parameter, extinction coefficient and scattering albedo. Using DOM/FDM for the solution to the radiative transfer equation and the energy equation, David et al. [3] investigated transient heat transfer involving radiation and conduction in a 2-D non-gray purely absorbing glass. Using FVM/LBM, the transient conduction–radiation heat transfer in 1-D planar and 2-D rectangular geometries was solved, and effects of the scattering albedo, the conduction–radiation parameter and the boundary emissivity were analyzed [4].

Most of the previous work on radiative heat transfer only considered isotropic scattering or non-scattering in the semitransparent material. However, it is well known that scattering of thermal radiation by real particles, fibers, or impurities in a medium is by no means isotropic and that the anisotropic scattering can play a significant role on overall heat transfer. Consequently it is necessary to carry on an investigation in radiative heat transfer within

* Corresponding author. Tel.: +86 451 86412028; fax: +86 451 86413208.
E-mail address: tanheping77@yahoo.com.cn (H.-P. Tan).

0017-9310/$ - see front matter © 2008 Elsevier Ltd. All rights reserved.
doi:10.1016/j.ijheatmasstransfer.2008.04.054

Nomenclature

C_n specific volume heat capacity of the layer n, $=c_n\rho_n$, J m^{-3} K^{-1}
FV_n a direct exchange area of V_i vs V_i in the nth layer, equal to $FV_n = 4\kappa_n\Delta x_n - 2[1 - E_3(\kappa_n\Delta x_n)]$, n = 1, 2
h_1, h_2 convective heat transfer coefficient at surfaces of S_1 and S_2, respectively, W m^{-2} K^{-1}
H_1, H_2 convection–radiation parameter, $H_1 = h_1/\sigma T_r^3$ and $H_2 = h_2/\sigma T_r^3$
L thickness of the composite medium, m
k_n thermal conductivity of the nth layer, W m^{-1} K^{-1}, n = 1, 2
k_{ie}, k_{iw} harmonic mean thermal conductivity at interface ie and iw of control volume i, respectively
N_n $k_n/(4\sigma T_r^3 L)$, conduction–radiation parameter of the nth layer, n = 1, 2
N_{cv1}, N_{cv2} number of control volumes in the first layer and the second layer, respectively
M_t total number of control volumes of the composite medium
n_i refractive index of the control volume i; when $i \leqslant N_{cv1}$, n_i is equal to the refractive index of the first layer, and when $i > N_{cv1}$, n_i is equal to the refractive index of the second layer
n_n refractive index of the nth layer, n = 1, 2
S_u, S_v black surfaces, $S_{-\infty}$ and $S_{+\infty}$, respectively
S_1, S_2 boundary surfaces
$S_{-\infty}$, $S_{+\infty}$ black surfaces representing the surroundings
(S_uS_v), (S_uV_j), (V_jS_u), (V_iV_j) absorbing RTCs of surface vs surface, surface vs volume, volume vs surface and volume vs volume
$[S_uS_v]$, $[S_uV_j]$, $[V_jS_u]$, $[V_iV_j]$ scattering RTCs of surface vs surface, surface vs volume, volume vs surface and volume vs volume
T absolute temperature, K
T_{g1}, T_{g2} gas temperatures for convection, K
T_r, T_0 reference temperature, initial temperature, K
t physical time, s
t^* dimensionless time, $(4\sigma T_r^3/C_nL)t$, only for the case of C_n = constant
x_i^j normal distance between element i and element j, m
β_n a common ratio of geometric progression when the radiation transfers in the nth layer, n = 1, 2
β_{ij} a common ratio of geometric progression when the radiation enters the jth layer from the ith layer and transfers inside the two-layer medium
γ_{ij} transmissivity at interface when radiation enters the j layer from the i layer, equal to $1 - \rho_{ij}$
Δt time interval, s
Δx_n thickness of each control volume of the nth layer, m
δ_{ij} a Dirac functor; if $i = j$, then δ_{ij} = 1, and if $i \neq j$, then δ_{ij} = 0
$(\delta x)_{ie}$, $(\delta x)_{iw}$ distance between nodes i and i + 1 and between i and $i - 1$, respectively
η_n $1 - \omega_n$, n = 1, 2
$\Theta_n^q(\theta)$, $\Theta_n^h(\theta)$ radiative energy distribution function of forward scattering and backward scattering respectively, for the nth layer, n = 1,2
θ, θ_s incident angle, scattering angle, rad
θ_{ij} refractive angle when radiation enters the j layer from the i layer
κ_n extinction coefficient of the nth layer, m^{-1}, n = 1, 2
ρ_{ij} reflectivity at interface when radiation enters the j layer from the i layer
σ Stefan–Boltzmann constant, =5.6696 $\times$ 10^{-8} W m^{-2} K^{-4}
Φ_n scattering phase function of the nth layer, n = 1, 2
Φ_i^r radiative heat source of the control volume i
ω_n scattering albedo of the nth layer, n = 1, 2

Subscripts
$\parallel$, $\perp$ component for parallel and perpendicular polarization, respectively
ie,iw right and left interface of control volume i
$-\infty$, $+\infty$ black surfaces $S_{-\infty}$ and $S_{+\infty}$, respectively

Superscripts
b,f,t incidence radiation from negative, positive and both direction relative to the x axis, respectively
h, q backward scattering and forward scattering relative to the incident direction, respectively
r radiation

anisotropic scattering participating medium. Much attention has been focused by many researchers on the problem [5–19].

Using the zone method, Goyheneche and Sacadura [7] established a new explicit matrix relation for the calculation of the total exchange areas (TEA) in emitting, absorbing and linearly anisotropic scattering semitransparent medium with black surfaces. Chai [9] presented a FVM to calculate transient radiative transfer in two-dimensional irregularly shaped enclosures with anisotropic scattering. Elghazaly [16] used the Galerkin-iterative technique to solve the coupled conductive–radiative transfer problem in a slab with two homogeneous layers of linearly anisotropic scattering with specularly reflecting boundaries and analyzed the effects of phase functions and anisotropic scattering coefficient on heat fluxes. Reflectivity was supposed to be zero in Ref. [16]. Zhou et al. [17] adopted the DRESOR method to deal with the radiative transfer in an anisotropic scattering, emitting, absorbing, plane-parallel medium with opaque surfaces, analyzing the effects of anisotropic scattering coefficient, scattering albedo and optical thickness. Asllanaj et al. [19] investigated transient radiative–conductive heat transfer in a fibrous medium with anisotropic optical properties using two-flux method/FEM for the solution to the radiative transfer equation and the energy equation.

The RTNAM was firstly proposed by Tan and Lallemand [20] and its advantage is that when solving radiative transfer equation, the radiative intensity does not need to be dispersed along the space coordinate, and the solid angle is not dispersed but is directly integrated. Thus, false scattering and ray effect will not exist in the method. So, the accuracy of this method is high in theory. Sadooghi et al. [21,22] and Sharbati et al. [23] adopted the method for the solution to the radiative transfer and investigated the coupled heat transfer in a purely absorbing ceramic layer [21,22] and a cellulose acetate layer [23]. Tan et al. [24,25] developed a two-layer [24] and a multilayer [25] radiative transfer model using RTNAM and solved the transient coupled heat transfer. Scattering was not considered in Refs. [21–23] and anisotropic scattering was not considered in Refs. [24,25]. After that, using this method, Tan et al. [26] built a radiative heat transfer model for an anisotropic scattering layer.

Present work develops a radiative transfer model for a two-layer composite with anisotropic scattering using the RTNAM. In this paper, RTCs (radiative transfer coefficients) include all information about the radiative transfer, and they are deduced by the ray-tracing method. Local radiative heat source in the energy equation is expressed in terms of RTCs and is deduced using the nodal-analyzing method. Semitransparent interfaces between two layers and between the composite and surroundings are considered. Specular reflectivity is determined by Fresnel's law and Snell's law. Total reflection criterion is proposed to settle the complicated total reflection problem at semitransparent interfaces which will result in integral singularity problem at the critical angle. The treatment is different from that proposed by Tan et al. [25], and it will not introduce any errors to results. Effects of conduction–radiation parameter, scattering albedo and refractive index on coupled heat transfer are analyzed.

2. Physical model and basic equations

A two-layer composite geometry with thickness of L under consideration is shown in Fig. 1. Both boundary surfaces of the geometry are semitransparent and specular, and contained medium is absorbing, emitting and anisotropic scattering. The two-layer geometry is irradiated by two black surfaces $S_{-\infty}$ and $S_{+\infty}$, indicating the environment of temperatures $T_{-\infty}$ and $T_{+\infty}$, respectively. Between $S_1$and $S_{-\infty}$ and between S_2 and $S_{+\infty}$ are convective gases with temperatures of T_{g1} and T_{g2}. Along the geometry thickness, the composite is divided into M_t control volumes, and the total number of nodes is $M_t + 2$, with node 0 locating S_1 and node $M_t + 1$ locating S_2. The number of control volumes of the left layer is N_{cv1}, and that of the right layer is N_{cv2}. The thermophysical and optical properties in each layer are different.

According to Fig. 1, in a fully implicit discrete format, the transient energy equation of coupled radiation and conduction, between the time intervals t and $t + \Delta t$, is written as

$$C_n\Delta x_n\frac{T_i^{m+1}-T_i^m}{\Delta t}=\frac{k_{ie}^{m+1}(T_{i+1}^{m+1}-T_i^{m+1})}{(\delta x)_{ie}}-\frac{k_{iw}^{m+1}(T_i^{m+1}-T_{i-1}^{m+1})}{(\delta x)_{iw}}+\Phi_i^{r,m+1} \tag{1}$$

where node i locates in the nth layer of the composite, and Φ_i^r is the radiative source of control volume i. By the nodal-analyzing method, for the gray medium, Φ_i^r can be expressed as

$$\begin{aligned}\Phi_i^r=&\ \sigma(n_{+\infty}^2[S_{+\infty}V_i]_{t-t}T_{+\infty}^4-n_i^2[V_iS_{+\infty}]_{t-t}T_i^4)\\&+\sigma\sum_{j=1}^{M_t}(n_j^2[V_jV_i]_{t-t}T_j^4-n_i^2[V_iV_j]_{t-t}T_i^4)\\&+\sigma(n_{-\infty}^2[S_{-\infty}V_i]_{t-t}T_{-\infty}^4-n_i^2[V_iS_{-\infty}]_{t-t}T_i^4)\end{aligned} \tag{2}$$

where such as $[S_{+\infty}V_i]$, $[V_iV_j]$, $[S_{-\infty}\ V_i]$ and so on are RTCs, deduced by the ray-tracing method.

The discrete boundary condition at semitransparent boundary surface S_1 is as follows:

$$2k_1(T_1-T_{S_1})/\Delta x_1=h_1(T_{S_1}-T_{g1}) \tag{3}$$

From Eq. (1), major difficulty in coupled radiative–conductive heat transfer problem is the solution to the local radiative source Φ_i^r, and the key to solve Φ_i^r, according to Eq. (2), is in deducing the RTCs.

3. Radiative transfer coefficients

RTC of element i (surface or control volume) with respect to element j is defined as quotient of the radiative energy absorbed by element j to the radiative energy emitted by element i. $[V_iV_j]_{t-t}$ is taken as an example to illustrate the deduction of RTCs. From Ref. [26], the deduction of $[V_iV_j]_{t-t}$ must start with the deduction of $(V_iV_j)_{t-t}^f$, $(V_iV_j)_{t-t}^b$, $(V_i\ V_j)_{t-t}$, $(V_iV_j)_{t-t}^{ff}$, $(V_iV_j)_{t-t}^{fb}$, $(V_iV_j)_{t-t}^{bf}$ and $(V_iV_j)_{t-t}^{bb}$. $[V_iV_j]_{t-t}$ is called as the scattering RTC, $(V_iV_j)_{t-t}$ is called as the absorbing RTC, $(V_iV_j)_{t-t}^f$ and $(V_iV_j)_{t-t}^b$ are called as the directional incidence RTCs, and $(V_iV_j)_{t-t}^{ff}$, $(V_iV_j)_{t-t}^{fb}$, $(V_iV_j)_{t-t}^{bf}$ and $(V_iV_j)_{t-t}^{bb}$ are called as the directional scattering RTCs. Superscript of the directional incidence RTC denotes the direction of radiative incidence on the second control volume V_j; The first superscript of the directional scattering RTC denotes the direction of radiative incidence on the second control volume V_i, and the second superscript denotes the direction of radiative incidence on the second control volume V_j. Superscript "f" denotes the positive direction of x-axis, and superscript "b" denotes the negative direction of x-axis. In the following deduction, symbol $\mathbf{F}_{A,n}^B$, denoting a single-layer radiative transfer model, determined in Appendix A, is used to denote the ratio of the radiative energy received by the control volume or interface B to that emitted by the control volume or interface A in the energy transfer process in the nth layer. FV_n is a direct exchange area of V_i vs V_i in the nth layer, equal to $FV_n = 4\kappa_n\Delta x_n - 2[1 - E_3(\kappa_n\Delta x_n)]$, $n = 1,\ 2$. For convenience subscript "$t - t$" denoting semitransparent surfaces are omitted.

3.1. Deduction of the absorbing and the directional incidence RTCs

The absorbing RTC (V_iV_j) includes two parts: the positive incidence RTC $(V_iV_j)^f$ and the negative incidence RTC $(V_iV_j)^b$, that is

$$(V_iV_j)=(V_iV_j)^f+(V_iV_j)^b \tag{4}$$

(1) If $i \leqslant N_{cv1}$ and $j \leqslant N_{cv1}$, then

$$\begin{aligned}(V_iV_j)^f=&\ 2\int_0^{\pi/2}f\_\mathbf{F}_{V_i,1}^{V_j}(\theta)\sin\theta\cos\theta\,d\theta\\&+2\int_0^{\pi/2}\frac{\mathbf{F}_{V_i,1}^{P}(\theta)\gamma_{12}(\theta)\mathbf{F}_{P,2}^{P}(\theta_{12})\gamma_{21}(\theta_{12})f\_\mathbf{F}_{P,1}^{V_j}(\theta)}{1-\beta_{12}}\sin\theta\cos\theta\,d\theta\\&+0.5\delta_{ij}FV_1\end{aligned} \tag{5a}$$

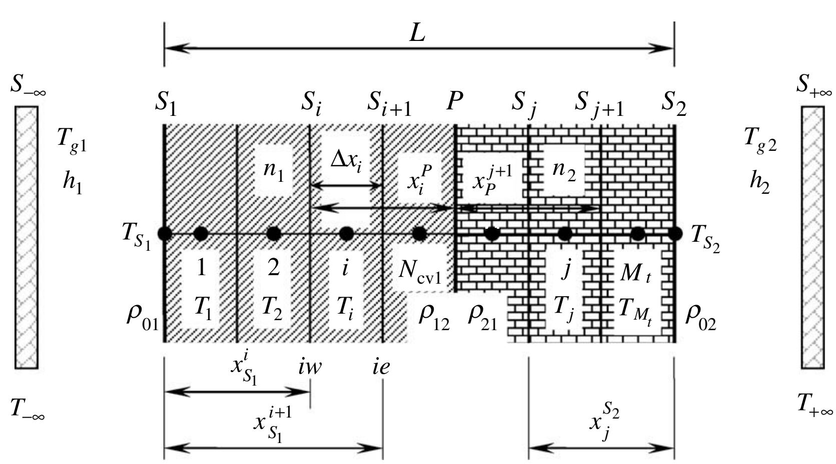

Fig. 1. Discrete physical model.

$$(V_iV_j)^b = 2\int_0^{\pi/2} b\_\mathbf{F}_{V_i,1}^{V_j}(\theta)\sin\theta\cos\theta\,\mathrm{d}\theta + 2\int_0^{\pi/2} \frac{\mathbf{F}_{V_i,1}^{P}(\theta)\gamma_{12}(\theta)\mathbf{F}_{P,2}^{P}(\theta_{12})\gamma_{21}(\theta_{12})b\_\mathbf{F}_{P,1}^{V_j}(\theta)}{1-\beta_{12}}\sin\theta\cos\theta\,\mathrm{d}\theta + 0.5\delta_{ij}FV_1 \tag{5b}$$

(2) If $i \leqslant N_{cv1}$ and $N_{cv1} < j \leqslant N_{cv1} + N_{cv2}$, then

$$(V_iV_j)^f = 2\int_0^{\pi/2} \frac{\mathbf{F}_{V_i,1}^{P}(\theta)\gamma_{12}(\theta)f\_\mathbf{F}_{P,2}^{V_j}(\theta_{12})}{1-\beta_{12}}\sin\theta\cos\theta\,\mathrm{d}\theta \tag{6a}$$

$$(V_iV_j)^b = 2\int_0^{\pi/2} \frac{\mathbf{F}_{V_i,1}^{P}(\theta)\gamma_{12}(\theta)b\_\mathbf{F}_{P,2}^{V_j}(\theta_{12})}{1-\beta_{12}}\sin\theta\cos\theta\,\mathrm{d}\theta \tag{6b}$$

(3) If $N_{cv1} < i \leqslant N_{cv1} + N_{cv2}$ and $N_{cv1} < j \leqslant N_{cv1} + N_{cv2}$, then

$$(V_iV_j)^f = 2\int_0^{\pi/2} f\_\mathbf{F}_{V_i,2}^{V_j}(\theta)\sin\theta\cos\theta\,\mathrm{d}\theta + 2\int_0^{\pi/2} \frac{\mathbf{F}_{V_i,2}^{P}(\theta)\gamma_{21}(\theta)\mathbf{F}_{P,1}^{P}(\theta_{21})\gamma_{12}(\theta_{21})f\_\mathbf{F}_{P,2}^{V_j}(\theta)}{1-\beta_{21}}\sin\theta\cos\theta\,\mathrm{d}\theta + 0.5\delta_{ij}FV_2 \tag{7a}$$

$$(V_iV_j)^b = 2\int_0^{\pi/2} b\_\mathbf{F}_{V_i,2}^{V_j}(\theta)\sin\theta\cos\theta\,\mathrm{d}\theta + 2\int_0^{\pi/2} \frac{\mathbf{F}_{V_i,2}^{P}(\theta)\gamma_{21}(\theta)\mathbf{F}_{P,1}^{P}(\theta_{21})\gamma_{12}(\theta_{21})b\_\mathbf{F}_{P,2}^{V_j}(\theta)}{1-\beta_{21}}\sin\theta\cos\theta\,\mathrm{d}\theta + 0.5\delta_{ij}FV_2 \tag{7b}$$

(4) If $N_{cv1} < i \leqslant N_{cv1} + N_{cv2}$ and $j \leqslant N_{cv1}$, then

$$(V_iV_j)^f = 2\int_0^{\pi/2} \frac{\mathbf{F}_{V_i,2}^{P}(\theta)\gamma_{21}(\theta)f\_\mathbf{F}_{P,1}^{V_j}(\theta_{21})}{1-\beta_{21}}\sin\theta\cos\theta\,\mathrm{d}\theta \tag{8a}$$

$$(V_iV_j)^b = 2\int_0^{\pi/2} \frac{\mathbf{F}_{V_i,2}^{P}(\theta)\gamma_{21}(\theta)b\_\mathbf{F}_{P,1}^{V_j}(\theta_{21})}{1-\beta_{21}}\sin\theta\cos\theta\,\mathrm{d}\theta \tag{8b}$$

In Eqs. (5)–(8), β_{ij} (i,j = 1, 2, $i \neq j$) is a common ratio of geometric progression when the radiation enters the jth layer from the ith layer and transfers inside the two-layer medium, equal to $\gamma_{ij}(\theta)\mathbf{F}_{P,j}^{P}(\theta_{ij})\gamma_{ji}(\theta_{ij})\mathbf{F}_{P,i}^{P}(\theta)$, and θ_{ij} is the refractive angle, decided by the Snell's law, equal to $\arcsin(n_i\sin\theta/n_j)$.

3.2. Deduction of the directional scattering RTCs

For the positive direction of radiative incidence on V_i, $(V_iV_j)^{ft}$ is used to denote the quotient of the radiative energy absorbed by V_j to the radiative energy scattered by V_i; and for the negative direction of radiative incidence on V_i, $(V_i\ V_j)^{bt}$ is used to denote the quotient of the radiative energy absorbed by V_j to the radiative energy scattered by V_i. Both $(V_iV_j)^{ft}$ and $(V_iV_j)^{bt}$ include two parts: the part of positive incidence on V_j and the part of negative incidence on V_j. So, we have

$$(V_iV_j)^{ft} = (V_iV_j)^{ff} + (V_iV_j)^{fb} \tag{9a}$$

$$(V_iV_j)^{bt} = (V_iV_j)^{bf} + (V_iV_j)^{bb} \tag{9b}$$

The deduction of $(V_iV_j)^{ff}$ is given as follows:

(1) For the case of $i < j \leqslant N_{cv1}$.
For the positive direction of radiative incidence on V_i, according to Fig. 2, when $i < j \leqslant N_{cv1}$, the radiation scattered by V_i gets to V_j in four paths: one part forwardly scattered by V_i directly gets to V_j; one part backwardly scattered by V_i firstly gets to S_1, and after being reflected, it gets to V_j; one

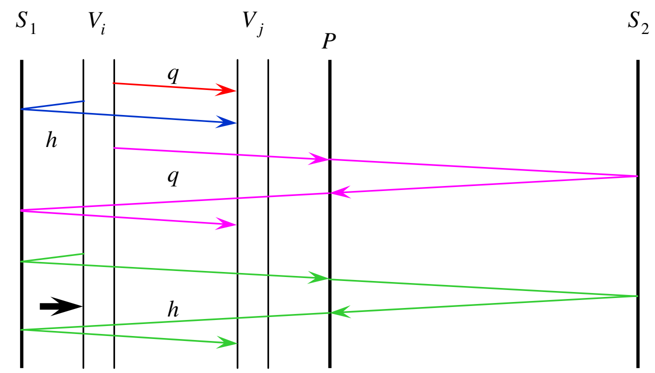

Fig. 2. Four transferring paths from V_i scattered to V_j in forward direction, $i < j \leqslant N_{cv1}$.

part forwardly scattered by V_i firstly gets to interface P, and after penetrating through P, it transfers in the second layer and gets back to P, and after penetrating through P again, it transfers in the first layer and finally gets to V_j in positive direction; and one part backwardly scattered by V_i firstly gets to S_1, and after being reflected, it reaches P, and after penetrating through P, it transfers in the second layer and gets back to P, and after penetrating through P again, it transfers in the first layer and finally gets to V_j in positive direction. That is, $(V_iV_j)^{ff}$ is the sum of its four parts

$$(V_iV_j)^{ff} = 2\int_0^{\pi/2} \Gamma_1(V_i \to V_j)\Theta_1^{q}(\theta)\sin\theta\cos\theta\,\mathrm{d}\theta + 2\int_0^{\pi/2} \Gamma_1(V_i \to S_1 \to V_j)\Theta_1^{h}(\theta)\sin\theta\cos\theta\,\mathrm{d}\theta + 2\int_0^{\pi/2} \frac{b\_\mathbf{F}_{P,1}^{V_i}(\theta)\Theta_1^{q}(\theta)\gamma_{12}(\theta)\mathbf{F}_{P,2}^{P}(\theta_{12})\gamma_{2,1}(\theta_{12})f\_\mathbf{F}_{P,1}^{V_j}(\theta)}{1-\beta_{12}} \times \sin\theta\cos\theta\,\mathrm{d}\theta + 2\int_0^{\pi/2} \frac{f\_\mathbf{F}_{P,1}^{V_i}(\theta)\Theta_1^{h}(\theta)\gamma_{12}(\theta)\mathbf{F}_{P,2}^{P}(\theta_{12})\gamma_{21}(\theta_{12})f\_\mathbf{F}_{P,1}^{V_j}(\theta)}{1-\beta_{12}} \times \sin\theta\cos\theta\,\mathrm{d}\theta \tag{10}$$

where $\Gamma_1(V_i \to V_j)$ and $\Gamma_1(V_i \to S_1 \to V_j)$ are radiative transfer functions of the first layer for the paths $V_i \to V_j$ and $V_i \to S_1 \to V_j$, determined in Appendix A.

(2) For the case of $j \leqslant i \leqslant N_{cv1}$.
According to Fig. 3, when $j \leqslant i \leqslant N_{cv1}$, by the similar analysis, the expression of $(V_iV_j)^{ff}$ is given by

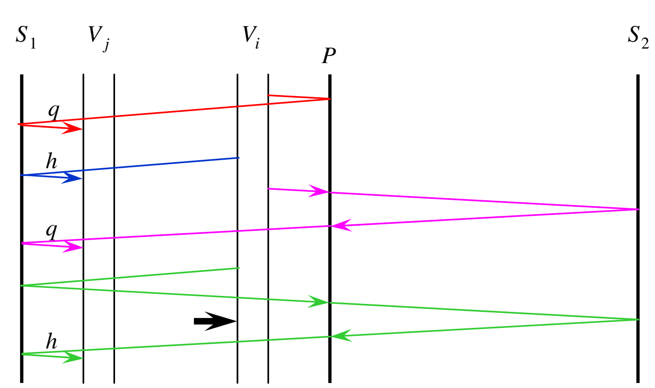

Fig. 3. Four transferring paths from V_i scattered to V_j in forward direction, $j \leqslant i \leqslant N_{cv1}$.

$$(V_iV_j)^{ff} = 0.5\delta_{ij}FV_1 + 2\int_0^{\pi/2}\Gamma_1(V_i \to P \to S_1 \to V_j)\Theta_1^q(\theta)\times\sin\theta\cos\theta\,\mathrm{d}\theta + 2\int_0^{\pi/2}\Gamma_1(V_i \to S_1 \to V_j)\Theta_1^h(\theta)\times\sin\theta\cos\theta\,\mathrm{d}\theta + 2\int_0^{\pi/2}\frac{b\_\mathbf{F}_{P,1}^{V_i}(\theta)\Theta_1^q(\theta)\gamma_{12}(\theta)\mathbf{F}_{P,2}^P(\theta_{12})\gamma_{21}(\theta_{12})f\_\mathbf{F}_{P,1}^{V_j}(\theta)}{1-\beta_{12}}\times\sin\theta\cos\theta\,\mathrm{d}\theta + 2\int_0^{\pi/2}\frac{f\_\mathbf{F}_{P,1}^{V_i}(\theta)\Theta_1^h(\theta)\gamma_{12}(\theta)\mathbf{F}_{P,2}^P(\theta_{12})\gamma_{21}(\theta_{12})f\_\mathbf{F}_{P,1}^{V_j}(\theta_i)}{1-\beta_{12}}\times\sin\theta\cos\theta\,\mathrm{d}\theta \quad (11)$$

where $\Gamma_1(V_i \to P \to S_1 \to V_j)$ is a radiative transfer function of the first layer for the path $V_i \to P \to S_1 \to V_j$, determined in Appendix A.

(3) For the case of $N_{cv1} < i < j \leqslant N_{cv1} + N_{cv2}$.
When $N_{cv1} < i < j \leqslant N_{cv1} + N_{cv2}$, in accordance with Eq. (10), making use of the symmetry relation, we may write

$$(V_iV_j)^{ff} = 2\int_0^{\pi/2}\Gamma_2(V_i \to V_j)\Theta_2^q(\theta)\sin\theta\cos\theta\,\mathrm{d}\theta + 2\int_0^{\pi/2}\Gamma_2(V_i \to P \to V_j)\Theta_2^h(\theta)\sin\theta\cos\theta\,\mathrm{d}\theta + 2\int_0^{\pi/2}\frac{b\_\mathbf{F}_{P,2}^{V_i}(\theta)\Theta_2^q(\theta)\gamma_{21}(\theta)\mathbf{F}_{P,1}^P(\theta_{21})\gamma_{12}(\theta_{21})f\_\mathbf{F}_{P,2}^{V_j}(\theta)}{1-\beta_{21}}\times\sin\theta\cos\theta\,\mathrm{d}\theta + 2\int_0^{\pi/2}\frac{f\_\mathbf{F}_{P,2}^{V_i}(\theta)\Theta_2^h(\theta)\gamma_{21}(\theta)\mathbf{F}_{P,1}^P(\theta_{21})\gamma_{12}(\theta_{21})f\_\mathbf{F}_{P,2}^{V_j}(\theta)}{1-\beta_{21}}\times\sin\theta\cos\theta\,\mathrm{d}\theta \quad (12)$$

Where, $\Gamma_2(V_i \to V_j)$ and $\Gamma_2(V_i \to P \to V_j)$ are radiative transfer functions of the second layer for the $V_i \to V_j$ and $V_i \to P \to V_j$, determined in Appendix A.

(4) For the case of $N_{cv1} < j \leqslant i \leqslant N_{cv1} + N_{cv2}$
When $N_{cv1} < j \leqslant i \leqslant N_{cv1} + N_{cv2}$, the deduction of $(V_iV_j)^{ff}$ is similar with that of the case of $j \leqslant i \leqslant N_{cv1}$, and making use of the symmetry relation, we have

$$(V_iV_j)^{ff} = 0.5\delta_{ij}FV_2 + 2\int_0^{\pi/2}\Gamma_2(V_i \to S_2 \to P \to V_j)\Theta_2^q(\theta)\times\sin\theta\cos\theta\,\mathrm{d}\theta + 2\int_0^{\pi/2}\Gamma_2(V_i \to P \to V_j)\Theta_2^h(\theta)\sin\theta\cos\theta\,\mathrm{d}\theta + 2\int_0^{\pi/2}\frac{b\_\mathbf{F}_{P,2}^{V_i}(\theta)\Theta_2^q(\theta)\gamma_{21}(\theta)\mathbf{F}_{P,1}^P(\theta_{21})\gamma_{12}(\theta_{21})f\_\mathbf{F}_{P,2}^{V_j}(\theta)}{1-\beta_{21}}\times\sin\theta\cos\theta\,\mathrm{d}\theta + 2\int_0^{\pi/2}\frac{f\_\mathbf{F}_{P,2}^{V_i}(\theta)\Theta_2^h(\theta)\gamma_{21}(\theta)\mathbf{F}_{P,1}^P(\theta_{21})\gamma_{12}(\theta_{21})f\_\mathbf{F}_{P,2}^{V_j}(\theta)}{1-\beta_{21}}\times\sin\theta\cos\theta\,\mathrm{d}\theta \quad (13)$$

where $\Gamma_2(V_i \to S_2 \to P \to V_j)$ is a radiative transfer function of the second layer for the path $V_i \to S_2 \to P \to V_j$, determined in Appendix A.

(5) For the case of $i \leqslant N_{cv1}$ and $N_{cv1} < j \leqslant N_{cv1} + N_{cv2}$.
When $i \leqslant N_{cv1}$ and $N_{cv1} < j \leqslant N_{cv1} + N_{cv2}$, as shown in Fig. 4, the energy scattered by V_i in the first layer transfers to V_j in the second layer in two ways. According to Fig. 4, we have

$$(V_iV_j)^{ff} = 2\int_0^{\pi/2}\frac{b\_\mathbf{F}_{P,1}^{V_i}(\theta)\Theta_2^q(\theta)\gamma_{12}(\theta)f\_\mathbf{F}_{P,2}^{V_j}(\theta_{12})}{1-\beta_{12}}\sin\theta\cos\theta\,\mathrm{d}\theta + 2\int_0^{\pi/2}\frac{f\_\mathbf{F}_{P,1}^{V_i}(\theta)\Theta_2^h(\theta)\gamma_{12}(\theta)f\_\mathbf{F}_{P,2}^{V_j}(\theta_{12})}{1-\beta_{12}}\sin\theta\cos\theta\,\mathrm{d}\theta \quad (14)$$

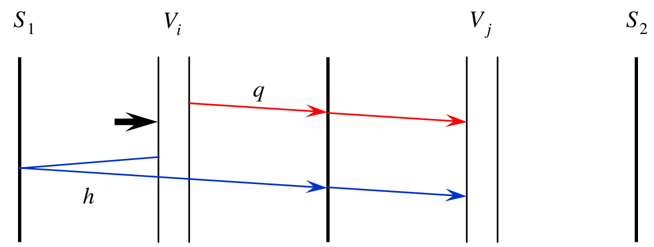

Fig. 4. Two transferring paths from V_i scattered to V_j in forward direction, $i \leqslant N_{cv1}$ and $j > N_{cv1}$.

(6) For the case of $N_{cv1} < i \leqslant N_{cv1} + N_{cv2}$ and $j \leqslant N_{cv1}$.

According to Fig. 5, when $N_{cv1} < i \leqslant N_{cv1} + N_{cv2}$ and $j \leqslant N_{cv1}$, $(V_iV_j)^{ff}$ can be obtained as follows

$$(V_iV_j)^{ff} = 2\int_0^{\pi/2}\frac{f\_\mathbf{F}_{P,2}^{V_i}(\theta)\Theta_2^h(\theta)\gamma_{21}(\theta)f\_\mathbf{F}_{P,1}^{V_j}(\theta_{21})}{1-\beta_{21}}\sin\theta\cos\theta\,\mathrm{d}\theta + 2\int_0^{\pi/2}\frac{b\_\mathbf{F}_{P,2}^{V_i}(\theta)\Theta_2^q(\theta)\gamma_{21}(\theta)f\_\mathbf{F}_{P,1}^{V_j}(\theta_{21})}{1-\beta_{21}}\sin\theta\cos\theta\,\mathrm{d}\theta \quad (15)$$

In Eqs. (10)–(15), $\Theta_n^q(\theta)$ and $\Theta_n^h(\theta)$ are distributing functions of energy scattered, defined as

$$\Theta_n^q(\theta) = \frac{\int_0^{\pi/2}\Phi_n(\theta,\theta_s)\,\mathrm{d}\theta_s}{\pi/2} \quad (16a)$$

$$\Theta_n^h(\theta) = \frac{\int_\pi^{-\pi/2}\Phi_n(\theta,\theta_s)\,\mathrm{d}\theta_s}{\pi/2} \quad (16b)$$

where Φ is the scattering phase function, θ is an angle of incidence, θ_s is an angle of scattering, subscript "n" denotes scattering happening in the nth layer, and superscript "q" denotes forward scattering, superscript "h" denotes backward scattering.

3.3. Determination of reflectivity at interfaces and treatment of total reflection

For the incidence of an unpolarized radiation, it can be divided into two parts: the parallel component and the perpendicular component. Tracing the two components separately could give the resultant expressions of the above RTCs, and their arithmetic average would finally give the directional incidence and the directional scattering RTCs, shown in Eqs. (5)–(8) and Eqs. (10)–(15), respectively.

When radiation transfers from the medium with refractive index of n_i towards the adjacent medium with refractive index of n_j, the reflectivity $\rho(\theta)_{ij}$ at the interface is [27] for parallel component

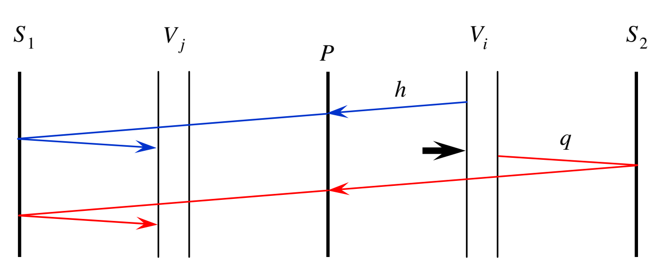

Fig. 5. Two transferring paths from V_i scattered to V_j in forward direction, $j \leqslant N_{cv1}$ and $i > N_{cv1}$.

$$\rho_{\parallel}(\theta)_{ij} = \left\{ \frac{(n_j/n_i)^2 \cos\theta - [(n_j/n_i)^2 - \sin^2\theta]^{0.5}}{(n_j/n_i)^2 \cos\theta + [(n_j/n_i)^2 - \sin^2\theta]^{0.5}} \right\}^2 \tag{17a}$$

and for perpendicular component,

$$\rho_{\perp}(\theta)_{ij} = \left\{ \frac{[(n_j/n_i)^2 - \sin^2\theta]^{0.5} - \cos\theta}{[(n_j/n_i)^2 - \sin^2\theta]^{0.5} + \cos\theta} \right\}^2 \tag{17b}$$

where the subscript "ij" indicates that radiation transfers from the medium with n_i towards the adjacent medium with n_j. In this paper, i, j = 0, 1, 2, and n_0 represents the refractive index of environment, equal to 1.

When $n_i < n_j$, total reflection will not occur at the interface, and $\rho(\theta)_{ij}$ determined by Eq. (17) is a continuous function; when $n_i > n_j$, total reflection will occur if $\theta \geqslant \theta_c$, and $\rho(\theta)_{ij}$ is a discontinuous function over the whole hemisphere space. With the number of medium layers increasing, total reflection will become very complex. The existence of total reflection will result in integral singularity problem in calculating the above RTCs. To overcome this problem, Luo et al. [25] proposed a technique based on division of the integral limit in terms of critical angles for total reflection at interfaces. While this treatment will introduce errors into results in theory due to dividing the integral limit into many intervals. We present a criterion for total reflection to solve the integral singularity problem with no errors introduced.

When radiation transfers from the medium having refractive index of n_i towards the adjacent medium having refractive index of n_j, the reflectivity at interfaces is determined as follows:

(1) If $n_i < n_j$, $\rho_{\parallel}(\theta)_{ij}$ and $\rho_{\perp}(\theta)_{ij}$ are determined by Eq. (17).
(2) If $n_i = n_j$, $\rho_{\parallel}(\theta)_{ij} = \rho_{\perp}(\theta)_{ij} = 0$.
(3) If $n_i > n_j$, when $\theta < \theta_c$, $\rho_{\parallel}(\theta)_{ij}$ and $\rho_{\perp}(\theta)_{ij}$ are determined by Eq. (17), and $\theta \geqslant \theta_c$, $\rho_{\parallel}(\theta)_{ij} = \rho_{\perp}(\theta)_{ij} = 1$.
(4) θ is the incident angle, and θ_c is the critical angle for total reflection, $\theta_c = \arcsin(n_j/n_i)$.

Making use of the criterion for total reflection, the integrands in Eqs. (5)–(8) and Eqs. (10)–(15) become continuous functions over the whole hemisphere space, which avoids the integral singularity, and they could be directly integrated. The technique proposed above does not divide the integral limit, so the errors will not be introduced into results. The criterion could be applied to the treatment of total reflection at interfaces in an arbitrary multilayer system.

3.4. Deduction of the scattering RTCs

According to the physical mechanism of radiative transfer, for the scattering medium, $[V_iV_j]$ includes two parts. One part is the quotient of energy leaving V_i that arrives at V_j directly without being scattered by the medium and is absorbed by V_j. The other part is the quotient of energy leaving V_i that firstly arrives at other control volumes, and after being scattered many times, arrives at V_j and is partly absorbed by V_j.

For the anisotropic scattering medium, energy scattered by control volumes is related to radiative incidence and scattering direction. According to the above analysis, making use of the RTCs deduced above, the scattering RTCs could be deduced. Before that, the absorbing RTCs, the directional incidence RTCs and the directional scattering RTCs must be normalized. For the RTC of control volume vs control colume, its coefficient of normalization is $1/(4\kappa_i\Delta x_n)$. In the following deduction, superscript "*" denotes the normalized parameter, subscripts "a" and "s" denote the absorbed and scattered parts, respectively. For convenience, first give four transferring expressions for energy scattered as follows.

When $n \geqslant 2$:

$$H(V_{l_{n+1}}V_{l_n})_a^{*ft} = \sum_{l_n=1}^{M_t}[(V_{l_{n+1}}V_{l_n})^{*ff}\omega_{l_n}H(V_{l_n}V_{l_{n-1}})_a^{*ft} + (V_{l_{n+1}}V_{l_n})^{*fb}\omega_{l_n}H(V_{l_n}V_{l_{n-1}})_a^{*bt}] \tag{18a}$$

$$H(V_{l_{n+1}}V_{l_n})_a^{*bt} = \sum_{l_n=1}^{M_t}[(V_{l_{n+1}}V_{l_n})^{*bf}\omega_{l_n}H(V_{l_n}V_{l_{n-1}})_a^{*ft} + (V_{l_{n+1}}V_{l_n})^{*bb}\omega_{l_n}H(V_{l_n}V_{l_{n-1}})_a^{*bt}] \tag{18b}$$

$$H(V_{l_{n+1}}V_{l_n})_s^{*ft} = \sum_{l_n=1}^{M_t}[(V_{l_{n+1}}V_{l_n})^{*ff}\omega_{l_n}H(V_{l_n}V_{l_{n-1}})_s^{*ft} + (V_{l_{n+1}}V_{l_n})^{*fb}\omega_{l_n}H(V_{l_n}V_{l_{n-1}})_s^{*bt}] \tag{18c}$$

$$H(V_{l_{n+1}}V_{l_n})_s^{*bt} = \sum_{l_n=1}^{M_t}[(V_{l_{n+1}}V_{l_n})^{*bf}\omega_{l_n}H(V_{l_n}V_{l_{n-1}})_s^{*ft} + (V_{l_{n+1}}V_{l_n})^{*bb}\omega_{l_n}H(V_{l_n}V_{l_{n-1}})_s^{*bt}] \tag{18d}$$

When $n = 1$:

$$H(V_{l_2}V_{l_1})_a^{*ft} = \sum_{l_1=1}^{M_t}[(V_{l_2}V_{l_1})^{*ff}\omega_{l_1}(V_{l_1}V_j)^{*ft}\eta_j + (V_{l_2}V_{l_1})^{*fb}\omega_{l_1}(V_{l_1}V_j)^{*bt}\eta_j] \tag{19a}$$

$$H(V_{l_2}V_{l_1})_a^{*bt} = \sum_{l_1=1}^{M_t}[(V_{l_2}V_{l_1})^{*bf}\omega_{l_1}(V_{l_1}V_j)^{*ft}\eta_j + (V_{l_2}V_{l_1})^{*bb}\omega_{l_1}(V_{l_1}V_j)^{*bt}\eta_j] \tag{19b}$$

$$H(V_{l_2}V_{l_1})_s^{*ft} = \sum_{l_1=1}^{M_t}[(V_{l_2}V_{l_1})^{*ff}\omega_{l_1}(V_{l_1}V_j)^{*ft}\omega_j + (V_{l_2}V_{l_1})^{*fb}\omega_{l_1}(V_{l_1}V_j)^{*bt}\omega_j] \tag{19c}$$

$$H(V_{l_2}V_{l_1})_s^{*bt} = \sum_{l_1=1}^{M_t}[(V_{l_2}V_{l_1})^{*bf}\omega_{l_1}(V_{l_1}V_j)^{*ft}\omega_j + (V_{l_2}V_{l_1})^{*bb}\omega_{l_1}(V_{l_1}V_j)^{*bt}\omega_j] \tag{19d}$$

(1) After the first scattering

$$[V_iV_j]_a^{*1st} = (V_iV_j)^*\eta_j \quad [V_iV_j]_s^{*1st} = (V_iV_j)^*\omega_j$$

(2) After the second scattering

$$[V_iV_j]_a^{*2nd} = [V_iV_j]_a^{*1st} + \sum_{l_1=1}^{M_t}[(V_iV_{l_1})^{*f}\omega_{l_1}(V_{l_1}V_j)^{*ft}\eta_j + (V_iV_{l_1})^{*b}\omega_{l_1}(V_{l_1}V_j)^{*bt}\eta_j]$$

$$[V_iV_j]_s^{*2nd} = \sum_{l_1=1}^{M_t}[(V_iV_{l_1})^{*f}\omega_{l_1}(V_{l_1}V_j)^{*ft}\omega_j + (V_iV_{l_1})^{*b}\omega_{l_1}(V_{l_1}V_j)^{*bt}\omega_j]$$

(3) After the third scattering

$$[V_iV_j]_s^{*3rd} = \sum_{l_2=1}^{M_t}[(V_iV_{l_2})^{*f}\omega_{l_2}H(V_{l_2}V_{l_1})_s^{*ft} + (V_iV_{l_2})^{*b}\omega_{l_2}H(V_{l_2}V_{l_1})_s^{*bt}]$$

$$[V_iV_j]_a^{*3rd} = [V_iV_j]_a^{*2nd} + \sum_{l_2=1}^{M_t}\{(V_iV_{l_2})^{*f}\omega_{l_2}\sum_{l_1=1}^{M_t}[(V_{l_2}V_{l_1})^{*ff} \times \omega_{l_1}(V_{l_1}V_j)^{*ft}\eta_j + (V_{l_2}V_{l_1})^{*fb}\omega_{l_1}(V_{l_1}V_j)^{*bt}\eta_j] + (V_iV_{l_2})^{*b}\omega_{l_2}\sum_{l_1=1}^{M_t}[(V_{l_2}V_{l_1})^{*bf}\omega_{l_1}(V_{l_1}V_j)^{*ft}\eta_j + (V_{l_2}V_{l_1})^{*bb}\omega_{l_1}(V_{l_1}V_j)^{*bt}\eta_j]\}$$

$$= [V_iV_j]_a^{*2nd} + \sum_{l_2=1}^{M_t}[(V_iV_{l_2})^{*f}\omega_{l_2}H(V_{l_2}V_{l_1})_a^{*ft} + (V_iV_{l_2})^{*b}\omega_{l_2}H(V_{l_2}V_{l_1})_a^{*bt}]$$

(4) After the $(n+1)$th scattering, if $\mathrm{Max}\sum_{j=1}^{M_t}[V_iV_j]_s^{*(n+1)\mathrm{th}} < 10^{-10}$, the redistributing of energy by anisotropic scattering is finished, and by induction, we have

$$[V_iV_j]_a^{*(n+1)\mathrm{th}} = [V_iV_j]_a^{*n\mathrm{th}} + \sum_{l_n=1}^{M_t}[(V_iV_{l_n})^{*f}\omega_{l_n}H(V_{l_n}V_{l_{n-1}})_a^{*ft} + (V_iV_{l_n})^{*b}\omega_{l_n}H(V_{l_n}V_{l_{n-1}})_a^{*bt}] \quad (20a)$$

$$[V_iV_j]_s^{*(n+1)th} = \sum_{l_n=1}^{M_t}[(V_iV_{l_n})^{*f}\omega_{l_n}H(V_{l_n}V_{l_{n-1}})_s^{*ft} + (V_iV_{l_n})^{*b}\omega_{l_n}H(V_{l_n}V_{l_{n-1}})_s^{*bt}] \quad (20b)$$

Considering emissive power of $4\kappa_i\eta_i\Delta x_n$ for V_i, the scattering RTC $[V_iV_j]$ could be finally found through the inverse operation,

$$[V_iV_j] = 4\kappa_i\eta_i\Delta x_n[V_iV_j]_a^{*(n+1)\mathrm{th}} \quad (21)$$

The rest scattering RTCs such as $[V_iS_{+\infty}]$, $[S_{+\infty}\ V_i]$, $[V_iS_{-\infty}]$ and $[S_{-\infty}V_i]$, could be obtained by similar deductions.

4. Validation of radiative transfer model and numerical method

4.1. Validation of radiative transfer coefficients

RTCs include all the information of radiative transfer, so the correctness of RTCs could be used to validate the radiative transfer model. From the reciprocity of radiative transfer and the conservation of radiative energy, RTCs must satisfy the relations of reciprocity and integrality.

Reciprocity relation

$$n_{S_u}^2[S_uV_i] = n_i^2[V_iS_u] \quad (22a)$$

$$n_{S_u}^2[S_uS_v] = n_{S_v}^2[S_vS_u] \quad (22b)$$

$$n_i^2[V_iV_j] = n_j^2[V_jV_i] \quad (22c)$$

Integrality relation

$$[V_iS_u] + [V_iS_v] + \sum_{j=1}^{M_t}[V_iV_j] = 4\kappa_i\eta_i\Delta x_n, \quad V_i \in \text{ the } n\text{th layer} \quad (23a)$$

$$[S_uS_u] + [S_uS_v] + \sum_{j=1}^{M_t}[S_uV_j] = \varepsilon_u \quad (23b)$$

From the calculation, Eqs. (22) and (23) are satisfied well with RTCs.

4.2. Comparison with other results from references

Attia [28] used a Galerkin-iterative technique and Liou et al. [29] used Nystrom method to solve the problem of radiative transfer in a two-region isotropic scattering slab with Fresnel interfaces and obtained the hemispherical reflectivity and transmissivity of the slab. In Ref. [28] refractive indices of the slab were assumed to be one, and Ref. [29] allowed refractive indices larger than one. In Ref. [29] the reflectivity at interfaces was determined by

$$\rho_{ij} = \frac{\rho_{\parallel}(\theta)_{ij} + \rho_{\perp}(\theta)_{ij}}{2} \quad (24)$$

For comparison, in our radiative transfer model the reflectivity at interfaces is also determined by Eq. (24) and the two polarized components of radiation are not traced separately.

According to Attia [28] and Wu and Liou [29], the hemispherical reflectivity and transmissivity of the two-layer slab are equal to RTCs $[S_{-\infty}S_{-\infty}]$ and $[S_{-\infty}S_{+\infty}]$ in quantity. Table 1 gives the

Table 1
Comparison with Ref. [28] and exact solution

Albedo		Optical thickness		Reflectivity			Transmissivity		
ω_1	ω_2	κ_1L_1	κ_2L_2	Ref. [28]	Exact[a]	This paper	Ref. [28]	Exact[a]	This paper
0.2	0.8	0.5	0.5	0.075338	0.07534	0.075335	0.313376	0.31338	0.313380
0.8	0.2	0.5	0.5	0.218436	0.21844	0.218429	0.313377	0.31338	0.313380
0.2	0.8	1.0	0.5	0.053409	0.05341	0.053407	0.166259	0.16626	0.166261
0.8	0.2	1.0	0.5	0.285692	0.28569	0.285686	0.213751	0.21375	0.213754
0.2	0.8	1.0	2.0	0.061625	0.06163	0.061624	0.055648	0.05565	0.055650
0.8	0.2	1.0	2.0	0.287419	0.28742	0.287413	0.034981	0.03498	0.034981

[a] Seen in Ref. [28].

Table 2
Comparison with Ref. [29]

Albedo		Optical thickness		Refractive index		Reflectivity		Transmissivity	
ω_1	ω_2	κ_1L_1	κ_2L_2	n_1	n_2	Ref. [29]	This paper	Ref. [29]	This paper
0.3	0.3	0.05	0.05	1.5	3.0	0.33077	0.330765	0.55863	0.558633
1.0	1.0	0.05	0.05	1.5	3.0	0.39544	0.395447	0.60455	0.604553
0.3	0.3	0.5	0.5	1.5	3.0	0.16057	0.160566	0.21130	0.211297
1.0	1.0	0.5	0.5	1.5	3.0	0.52266	0.522670	0.47733	0.477330
0.3	0.3	5.0	5.0	1.5	3.0	0.11245	0.112431	0.00002	0.000019
1.0	1.0	5.0	5.0	1.5	3.0	0.77008	0.769837	0.22991	0.230163
0.2	0.8	1.0	0.5	1.5	1.333	0.11350	0.113501	0.18584	0.185841
0.8	0.2	0.5	1.0	1.333	1.5	0.15372	0.153712	0.18584	0.185841
1.0	0.0	1.0	0.5	1.5	1.333	0.30520	0.305193	0.26519	0.265194
0.0	1.0	0.5	1.0	1.333	1.5	0.13583	0.135827	0.26519	0.265194
1.0	1.0	1.0	0.5	1.5	1.333	0.48603	0.486022	0.51397	0.513978
1.0	1.0	0.5	1.0	1.333	1.5	0.48603	0.486022	0.51397	0.513978

comparison with Ref. [28] and the exact solution and Table 2 gives the comparison with Ref. [29]. From Tables 1 and 2 we can see that the results of this paper accord very well with those of Ref. [28], the exact solution and Ref. [29], which demonstrates that the radiative transfer model of this paper is correct.

4.3. Numerical method

The radiative source term Φ_i^{r} is a nonlinear function of T_i, so it must be linearized as follows [30]:

$$\Phi_i^{\mathrm{r},m,n+1} = Sc_i^{m,n+1} + Sp_i^{m,n+1} T_i^{m,n+1} \tag{25}$$

with $Sc_i^{m,n+1} = \Phi_i^{\mathrm{r},m,n} - (\mathrm{d}\Phi_i^{\mathrm{r}}/\mathrm{d}T_i)^{m,n} T_i^{m,n}$, and $Sp_i^{m,n+1} = (\mathrm{d}\Phi_i^{\mathrm{r}}/\mathrm{d}T_i)^{m,n}$, where the superscript "m" denotes the "mth" time step, and "n" denotes the "nth" iteration in the "mth" time step. After linearization of the nonlinear term in Eq. (1), linear equations may be obtained and solved by TDMA (tri-diagonal matrix algorithm) to find temperatures at all nodes.

5. Transient coupled heat transfer

Considering a two-layer composite having two semitransparent surfaces with $L_1 = L_2 = 0.01$ m, $C_1 = C_2 = 1.5 \times 10^5\ \mathrm{J\,m^{-3}\,K^{-1}}$ and $\kappa_1 = 50\ \mathrm{m^{-1}}$, $\kappa_2 = 200\ \mathrm{m^{-1}}$, the effects of conduction–radiation parameter, scattering albedo and refractive index on transient coupled heat transfer are examined. Scattering phase functions of the two layers are taken as the combination of $\Phi_1(\theta,\theta_i) = 1 + \cos\theta\cos\theta_i$ and $\Phi_2(\theta,\theta_i) = 1 - \cos\theta\cos\theta_i$.

5.1. Effects of conduction–radiation parameter

Calculation parameters are taken as: $n_1 = n_2 = 2.0$, $\omega_1 = \omega_2 = 0.5$, $H_1 = 1.0$, $H_2 = 0$, $T_{-\infty} = T_{\mathrm{r}} = 1500$ K, and $T_0 = T_{\mathrm{g1}} = T_{\mathrm{g2}} = T_{+\infty} = 500$ K.

When the conduction–radiation parameter is small, $N_1 = N_2 = 0.0005$ and 0.005, there are two temperature peaks appearing in the composite medium in the transient, as shown in Fig. 6a and b. The first peak lies in the area close to the heating surface S_1, and is caused by the external radiation heating coupling with convection cooling in surroundings. The second peak existing in the area of the second layer close to the interface P is a result of the inhomogenous optical property of the composite medium.

Results for $N_1 = N_2 = 0.0005$ are plotted in Fig. 6a. In the first layer, after the first temperature peak, the temperature gradually falls along the thickness direction. This is because that the external radiation penetrating through the semitransparent surface S_1 is slowly attenuated by the first layer medium, thus the portion absorbed is a little, as a result of this layer with a small extinction coefficient of $\kappa_1 = 50\ \mathrm{m^{-1}}$. Most of the rest radiative energy entering into the second layer is immediately absorbed as a result of the extinction coefficient of this layer suddenly increasing to $\kappa_2 = 200\ \mathrm{m^{-1}}$ several times bigger than that of the first layer, which causes the temperature to rise rapidly in the area close to the interface P, and consequently causes the second temperature peak to appear therein. After the second peak, the radiative energy is gradually attenuated in the second layer, so that the temperature also decreases gradually along the thickness direction. Notice that the speed of the temperature decreasing in the second layer is faster than that in the first layer, that is to say the temperature gradient of the second layer is bigger than that of the first layer after the peaks. When temperature fields come into the steady state, the second temperature peak disappears and only the first temperature peak still exists.

The mechanism for the second temperature peak disappearance is now analyzed. With the evolving of the heat transfer, temperatures in the composite medium climb gradually as a result of the left external radiation heating on the whole medium. The area where the second peak appears absorbs the radiant energy from $S_{-\infty}$, and at the same time it transfers one part of energy to the neighboring regions by conduction and transfers the other part to the regions at lower temperatures by radiation. At the beginning of the transient, the area having temperature peak intensely absorbs heat so that the peak grows up and the temperature difference between the peak area and the surrounding areas increases. As a result of increase of peak, the absorption of radiative energy from the left external heat source is weakened in the peak area. As a result of increase of temperature difference, heat transfer from the peak area to other areas by conduction and radiation is intensified, that is to say the absorption of heat from the peak area gets more in other areas, which causes the temperature in the other areas to increase rapidly, and thus the temperature difference decreases, that is to say the temperature peak gets relatively small. At the steady state, the quantity of absorption of heat is equal to the quantity of dissipation of heat, so thermal equilibrium is achieved, and the second temperature peak completely disappears.

When $N_1 = N_2 = 0.005$, because of strengthening of conduction, temperature curves get smooth and the first temperature peak is very unconspicuous, as shown in Fig. 6b. When the conduction–radiation parameter increases to 0.05, temperature curves get more smooth and in the transient only one peak exists in the area close to the interface of the second layer, as plotted in Fig. 6c. In Fig. 6c, the temperature peak in the transient is caused by the inhomogenous distributing of extinction coefficients, and the peak appears at the steady state as a result of radiation heating and convective cooling. From Fig. 6a–e, we may observe that the first temperature peak is influenced mainly by the conduction–radiation parameter of the left layer having a heating surface: compared to the Fig. 6a, when $N_1 = 0.05$ and N_2 keeps unchanged, as shown in Fig. 6e, in the transient, due to the decrease of the radiation ratio, the first peak does not appear and only the second peak appear; until the second peak disappears at steady state, the first peak appears. From the above analysis, we may know that the first and the second temperature peaks are two sorts of temperature peaks having completely different characteristics: the first sort is caused by external radiation heating and environmental convective cooling, still existing in steady state; the second one is due to maximum of absorption of heat caused by inhomogeneous optical properties, only existing in transients of heat transfer.

5.2. Effects of scattering albedo

Calculation parameters are taken as: $n_1 = n_2 = 1.5$, $T_0 = 500$ K, $T_{\mathrm{r}} = 2000$ K, $T_{\mathrm{g1}} = T_{\mathrm{g2}} = 500$ K, $T_{-\infty} = 2000$ K, $T_{+\infty} = 1000$ K, $N_1 = N_2 = 0.0005$, and $H_1 = H_2 = 0$.

From Fig. 7a, we may see that temperature distributions in the composites having different combination of two scattering phase functions are almost the same, when scattering albedos of the two-layer composite are taken as small values such as $\omega_1 = \omega_2 = 0.1$. When scattering albedos increase to $\omega_1 = \omega_2 = 0.9$, the difference of the temperature distributions is relatively evident, as shown in Fig. 7b. In addition, for composites having homogeneous albedos, scattered quotient and absorbed quotient of radiative energy in two layers are the same, respectively, so the temperature fields in media are similar, as shown in Fig. 7a and b. While for composites having different albedos in each layer, scattered quotient and absorbed quotient of radiative energy in two layers are respectively different, so there are different trends of temperature evolution along the thickness direction in the composite media, as shown in Fig. 7c and d. For the composite having $\omega_1 = 0.1$ and $\omega_2 = 0.9$, the absorption coefficient of the left layer is $45m^{-1}$ and that of the right layer is $20\ \mathrm{m^{-1}}$, so the absorption of thermal radiation in the left layer is more intense than

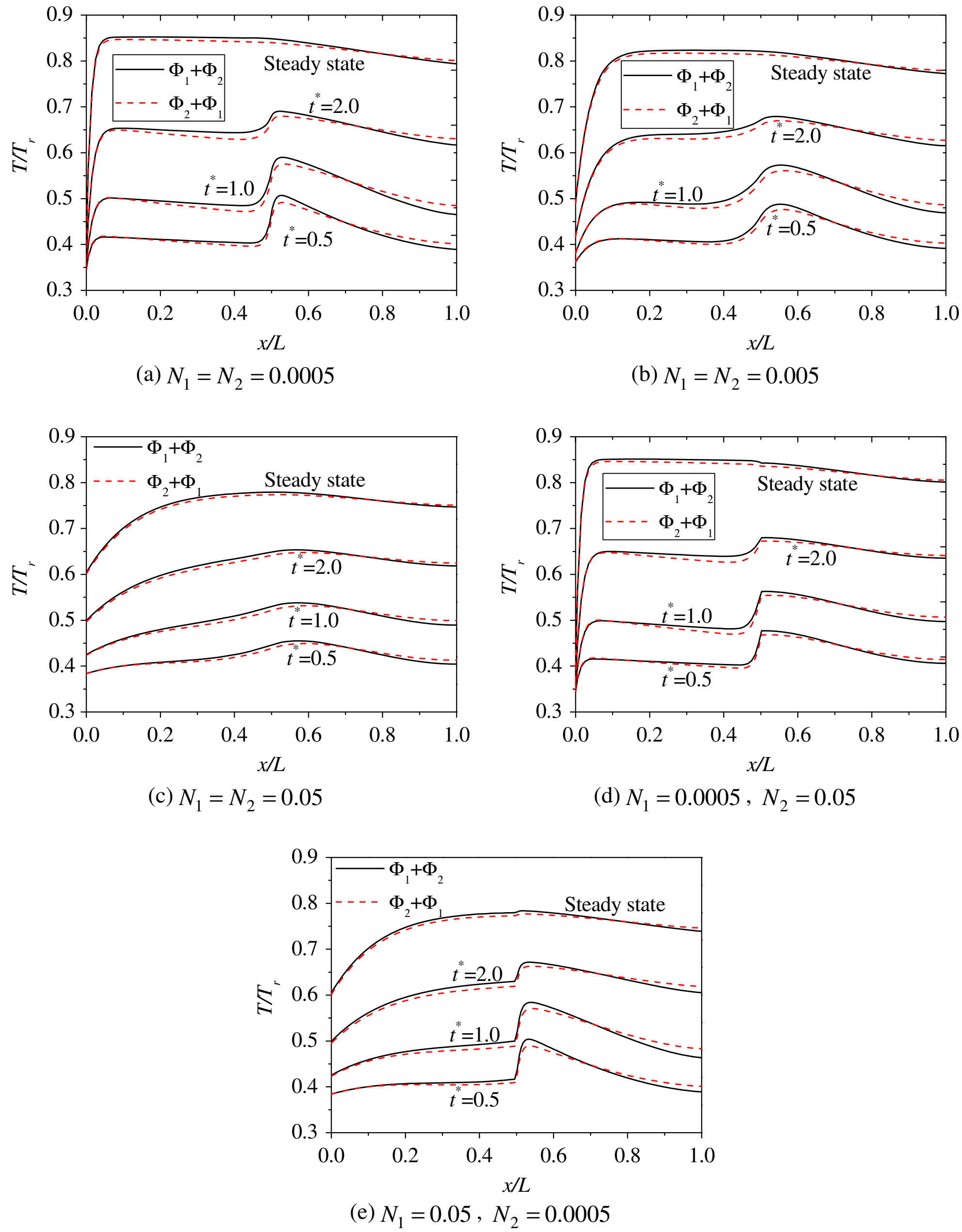

Fig. 6. Effects of conduction–radiation parameters on transient temperature fields in an anisotropic scattering composite layer.

that in the right layer, which causes the temperature to fall in the region close to interface *P*, and the temperature level of the left layer to be over that of the right layer, as shown in Fig. 7c. For the composite having $\omega_1 = 0.9$ and $\omega_2 = 0.1$, the results plotted in Fig. 7d shows that in the right layer the trend of the temperature changing is quite different from that shown in Fig. 7c. In this case the absorption coefficient of the right layer is 180 m^{-1}, much bigger than the absorption coefficient of 5 $m^{-1}$of the left layer, so the absorption of thermal radiation in the right layer is much more intense than that in the left layer, which causes the temperature to rise sharply in the region close to interface *P* and a sharp temperature peak to appear in the right layer. Hence one can see that in the transient a trend in the temperature change is mainly decided by the part of absorption in extinction coefficient instead of the part of scattering. The temperature peaks in Fig. 7a and b are caused by the inhomogeneous extinction coefficient resulting in maximum of absorption of heat in the peak areas. The temperature peaks shown in Fig. 7a, b and d are the second sort of peaks, not existing at a steady state. Without convection considered, the heating surface is not subject to convective cooling, so the first sort of temperature peaks does not exist in heat transfer. Compared with the case of transients, in steady state heat transfer is affected so little by the scattering and the temperature distribution is dominated mainly by the external heating conditions. So under the same external heating conditions the temperature curves of all the four cases in Fig. 7 in steady state show little difference although their scattering albedoes distributions are quite different.

5.3. Effects of refractive index

Calculation parameters are taken as: $\omega_1 = \omega_2 = 0.5$, $T_0 = 500$ K, $T_r = 1500$ K, $T_{g1} = T_{g2} = 500$ K, $T_{-\infty} = 1500$ K, $T_{+\infty} = 1000$ K, $N_1 = N_2 = 0.0005$, and $H_1 = 1.0$, $H_2 = 2.0$.

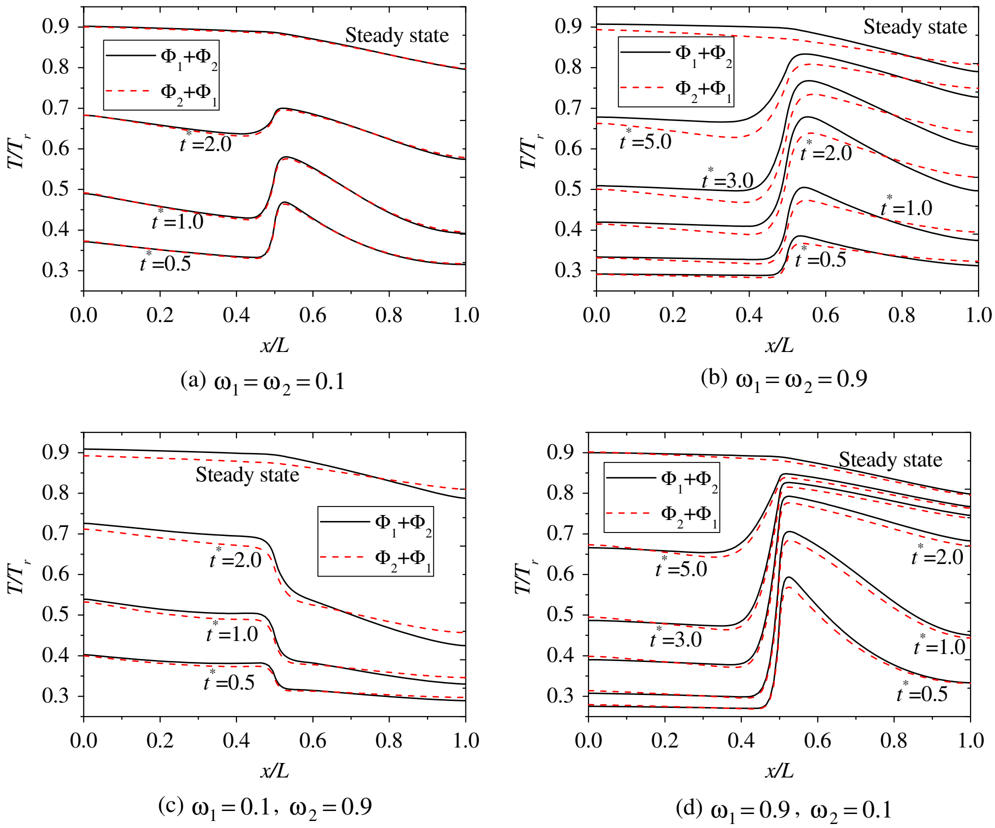

Fig. 7. Effects of scattering albedo on transient temperature fields in an anisotropic scattering composite layer.

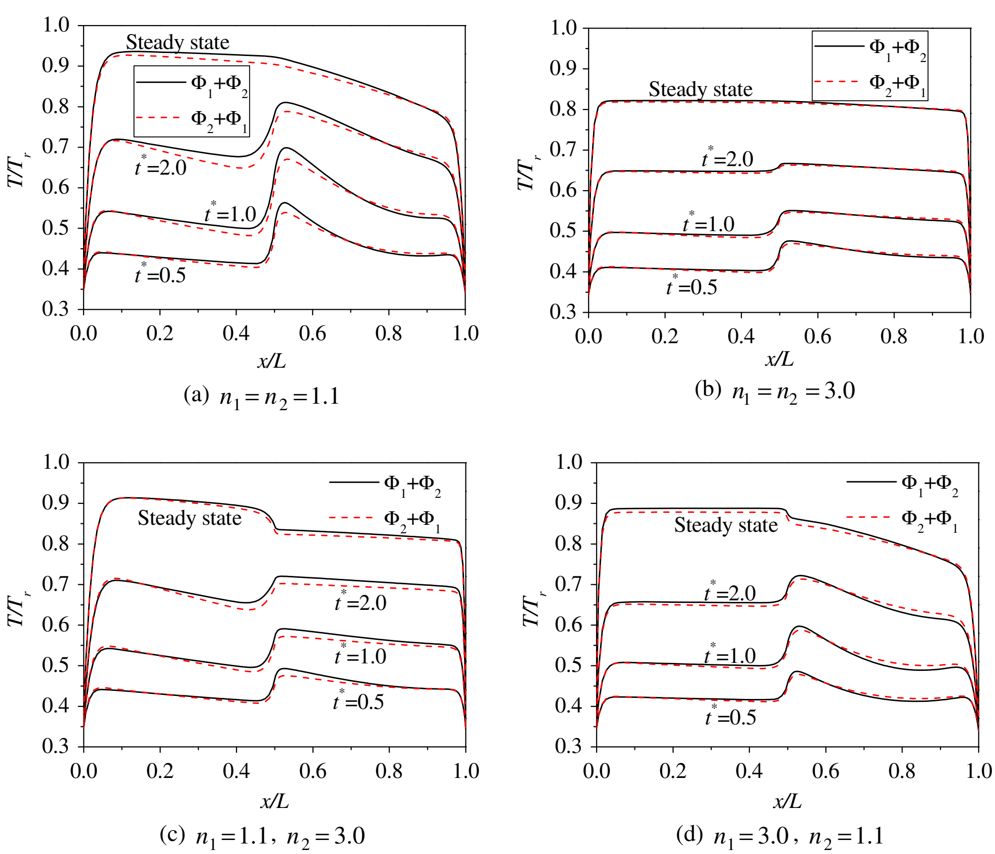

Fig. 8. Effects of refractive index on transient temperature fields in an anisotropic scattering composite layer.

For a semitransparent medium, thermal emission is proportional to the square of a refractive index, so the refractive index has a significant influence on transient heat transfer in the medium. In the medium having a smaller refractive index, the thermal emission is relatively weaker, and the thermal absorption is relatively stronger, so the average temperature level of the medium with a smaller refractive index remains higher compared to the medium having a bigger refractive index, as shown in Fig. 8. Compared to the medium having a smaller refractive index, the temperature peaks are smaller in the medium with a bigger refractive index under the condition for this calculation, as shown in Fig. 8a and b. From Fig. 8 we can also see that the temperature distributions in the medium with a bigger refractive index are more uniform. This because the larger the refractive index is, the stronger the total reflection is at the interface side facing the medium having the bigger refractive index, and the radiative energy reflected back to the medium causes a gentler temperature curves. For the composite having different refractive index in two layers, as shown in Fig. 8c and d, the temperature fields are decided by thermal emission of the medium and total reflection at interfaces together. Total reflection at interfaces and thermal emission are weak in the layer having a small refractive index, and total reflection at interfaces and thermal emission are strong in the layer having a big refractive index. Compared to Fig. 8a and b, from Fig. 8c and d one can see that the average temperature level in a medium layer depends mainly on the thermal emission of this layer medium, and total reflection at interfaces in this layer mainly causes its temperature fields to be gentler. Moreover, since two surfaces are all subject to external radiation heating and convective cooling together, two temperature peaks may appear in areas adjacent to the surfaces in the transient, as shown in Fig. 8, and they belong to the second sorts of peaks.

6. Conclusions

This paper developed a radiative transfer model using a ray-tracing/nodal-analyzing method for a two-layer composite medium with anisotropic scattering, and investigated the coupled radiative–conductive heat transfer, examining the effects of conduction–radiation parameters, scattering albedos and refractive indexes. From what has been discussed above, we may draw some conclusions as follows.

(1) Using the radiative transfer model for single layer, and combined with the concepts of directional incidence and directional scattering, radiative transfer coefficients are deduced for the anisotropic scattering composite medium with semitransparent surfaces by a ray-tracing method, and the radiative transfer model is developed for a two-layer anisotropic scattering medium.

(2) A more concise and precise criterion for total reflection occurring at interfaces is proposed in order to solve the complicated total reflection problem at semitransparent interfaces which will result in integral singularity problem at the critical angle. The general criterion will not introduce any errors into results and could be applied to the treatment of total reflection at interfaces in an arbitrary multilayer system.

(3) In a semitransparent medium having semitransparent surfaces, there are two sorts of temperature peaks appearing at transient heat transfer: one is caused by external radiation heating and environmental convection cooling, still existing in steady state; the other is due to maximum of absorption of heat caused by inhomogeneous optical properties (such as extinction coefficients, etc.), only existing in transients of heat transfer. Furthermore, the mechanism for disappearance of the second temperature peak at steady state is qualitatively analyzed.

(4) For a scattering medium, the absorption part and the scattering part of extinction coefficients have different effects on transient heat transfer, and the developmental tendency of transient temperatures in the medium is dominated mainly by the absorption part instead of the scattering part.

(5) The average temperature level in a medium layer depends mainly on the thermal emission of this layer medium, and total reflection at interfaces in this layer mainly causes its temperature fields to be gentler.

Acknowledgement

This research is supported by the Major Program of International Cooperation of National Natural Science Foundation of China (No. 50620120442), and the Key Project of National Natural Science Foundation of China (No. 50336010). The authors are indebted to them for their financial support.

Appendix A. Single-layer radiative transfer model

We are interested in the energy transfer process, in which the radiative energy emitted by an interface or a control volume propagates within the nth layer of a composite medium, and is reflected and absorbed many times until the energy becomes zero.

In the following deduction, $\beta_n(\theta)$ is a common ratio of geometric progression when the radiation transfers in the nth layer, equal to

$$\rho_{n0}(\theta)\rho_{nm}(\theta)\exp(-2\kappa_n L_n/\cos\theta)$$

where n, $m = 1, 2$, and $n \neq m$.

By tracing the transfer process for the radiative energy emitted by the interface P at the angle θ in the nth layer, we can obtain the following radiative energy quotient functions

$$\mathbf{F}^{P}_{P,n}(\theta) = \frac{\rho_{n0}(\theta)\exp(-2\kappa_n L_n/\cos\theta)}{1-\beta_n(\theta)} \tag{A.1}$$

$$f\_\mathbf{F}^{V_j}_{P,1}(\theta) = \frac{\rho_{10}(\theta)\exp[-\kappa_1(L_1 + x^j_{S_1})/\cos\theta][1-\exp(-\kappa_1\Delta x_1/\cos\theta)]}{1-\beta_1(\theta)} \tag{A.2a}$$

$$f\_\mathbf{F}^{V_j}_{P,2}(\theta) = \frac{\exp(-\kappa_2 x^j_P/\cos\theta)[1-\exp(-\kappa_2\Delta x_2/\cos\theta)]}{1-\beta_2(\theta)} \tag{A.2b}$$

$$b\_\mathbf{F}^{V_j}_{P,1}(\theta) = \frac{\exp(-\kappa_1 x^{j+1}_P/\cos\theta)[1-\exp(-\kappa_1\Delta x_1/\cos\theta)]}{1-\beta_1(\theta)} \tag{A.3a}$$

$$b\_\mathbf{F}^{V_j}_{P,2}(\theta) = \frac{\rho_{20}(\theta)\exp[-\kappa_2(L_2 + x^{j+1}_{S_2})/\cos\theta][1-\exp(-\kappa_2\Delta x_2/\cos\theta)]}{1-\beta_2(\theta)} \tag{A.3b}$$

where "f" denotes the positive incidence upon V_j, and "b" denotes the negative incidence upon V_j.

By tracing the transfer process for the radiative energy emitted by the control volume at the angle θ in the nth layer, we can obtain the following radiative energy quotient functions

$$\mathbf{F}^{P}_{V_j,n}(\theta) = f\_\mathbf{F}^{V_j}_{P,n}(\theta) + b\_\mathbf{F}^{V_j}_{P,n}(\theta) \tag{A.4}$$

If the radiative energy emitted by V_i reaches V_j in a positive direction, when $i < j$, we have

$$f\_\mathbf{F}^{V_j}_{V_i,1}(\theta) = \Gamma_1(V_i \to V_j) + \Gamma_1(V_i \to S_1 \to V_j) \tag{A.5}$$

$$f\_\mathbf{F}^{V_j}_{V_i,2}(\theta) = \Gamma_2(V_i \to V_j) + \Gamma_2(V_i \to P \to V_j) \tag{A.6}$$

where $\Gamma_1(V_i \to V_j)$ and $\Gamma_1(V_i \to S_1 \to V_j)$ are radiative transfer functions of the first layer for the paths $V_i \to V_j$ and $V_i \to S_1 \to V_j$, and $\Gamma_2(V_i \to V_j)$ and $\Gamma_2\ (V_i \to P \to V_j)$ are radiative transfer functions of the second layer for the $V_i \to V_j$ and $V_i \to P \to V_j$,

$$\Gamma_1(V_i \to V_j) = \frac{\exp(-\kappa_1 x^j_{i+1}/\cos\theta)[1-\exp(-\kappa_1\Delta x_1/\cos\theta)]^2}{1-\beta_1(\theta)} \quad \text{(A.7a)}$$

$$\Gamma_1(V_i \to S_1 \to V_j) = \frac{\rho_1 \exp[-\kappa_1(x^{S_1}_i + x^j_{S_1})/\cos\theta][1-\exp(-\kappa_1\Delta x_1/\cos\theta)]^2}{1-\beta_1(\theta)} \quad \text{(A.7b)}$$

$$\Gamma_2(V_i \to V_j) = \frac{\exp(-\kappa_2 x^j_{i+1}/\cos\theta)[1-\exp(-\kappa_2\Delta x_2/\cos\theta)]^2}{1-\beta_2(\theta)} \quad \text{(A.8a)}$$

$$\Gamma_2(V_i \to P \to V_j) = \frac{\rho_{21}(\theta)\exp[-\kappa_2(x^P_i + x^j_P)/\cos\theta][1-\exp(-\kappa_2\Delta x_2/\cos\theta)]^2}{1-\beta_2(\theta)} \quad \text{(A.8b)}$$

and when $i \geqslant j$, we have

$$f\_\mathbf{F}^{V_j}_{V_i,1}(\theta) = \Gamma_1(V_i \to P \to S_1 \to V_j) + \Gamma_1(V_i \to S_1 \to V_j) \quad \text{(A.9)}$$

$$f\_\mathbf{F}^{V_j}_{V_i,2}(\theta) = \Gamma_2(V_i \to S_2 \to P \to V_j) + \Gamma_2(V_i \to P \to V_j) \quad \text{(A.10)}$$

where $\Gamma_1(V_i \to S_1 \to V_j)$ and $\Gamma_2\ (V_i \to P \to V_j)$ are seen in Eqs. (A.7b) and (A.8b), and $\Gamma_1(V_i \to P \to S_1 \to V_j)$ and $\Gamma_2(V_i \to S_2 \to P \to V_j)$, as radiative transfer functions for the path $V_i \to P \to S_1 \to V_j$ in the first layer and the path $V_i \to S_2 \to P \to V_j$ in the second layer, are given by

$$\Gamma_1(V_i \to P \to S_1 \to V_j) = \frac{\rho_{10}(\theta)\rho_{12}(\theta)\exp\left[\frac{-\kappa_1(x^P_{i+1}+L_1+x^j_{S_1})}{\cos\theta}\right]\left[1-\exp\left(\frac{-\kappa_1\Delta x_1}{\cos\theta}\right)\right]^2}{1-\beta_1(\theta)} \quad \text{(A.11)}$$

$$\Gamma_2(V_i \to S_2 \to P \to V_j) = \frac{\rho_{20}(\theta)\rho_{21}(\theta)\exp\left[\frac{-\kappa_2(x^{S_2}_{i+1}+L_2+x^j_P)}{\cos\theta}\right]\left[1-\exp\left(\frac{-\kappa_2\Delta x_2}{\cos\theta}\right)\right]^2}{1-\beta_2(\theta)} \quad \text{(A.12)}$$

If the radiative energy emitted by V_i reaches V_j in a negative direction, when $i \leqslant j$, we have

$$b\_\mathbf{F}^{V_j}_{V_i,1}(\theta) = \Gamma_1(V_i \to P \to V_j) + \Gamma_1(V_i \to S_1 \to P \to V_j) \quad \text{(A.13)}$$

$$b\_\mathbf{F}^{V_j}_{V_i,2}(\theta) = \Gamma_2(V_i \to S_2 \to V_j) + \Gamma_2(V_i \to P \to S_2 \to V_j) \quad \text{(A.14)}$$

where $\Gamma_1(V_i \to P \to V_j)$, $\Gamma_1\ (V_i \to S_1 \to P \to V_j)$, $\Gamma_2(V_i \to S_2 \to V_j)$ and $\Gamma_2\ (V_i \to P \to S_2 \to V_j)$ are given by

$$\Gamma_1(V_i \to P \to V_j) = \frac{\rho_{12}(\theta)\exp[-\kappa_1(x^P_{i+1} + x^{j+1}_P)/\cos\theta][1-\exp(-\kappa_1\Delta x_1/\cos\theta)]^2}{1-\beta_1(\theta)} \quad \text{(A.15a)}$$

$$\Gamma_1(V_i \to S_1 \to P \to V_j) = \frac{\rho_{10}(\theta)\rho_{12}(\theta)\exp\left[\frac{-\kappa_1(x^{S_1}_i+L_1+x^{j+1}_P)}{\cos\theta}\right]\left[1-\exp\left(\frac{-\kappa_1\Delta x_1}{\cos\theta}\right)\right]^2}{1-\beta_1(\theta)} \quad \text{(A.15b)}$$

$$\Gamma_2(V_i \to S_2 \to V_j) = \frac{\rho_{20}(\theta)\exp[-\kappa_2(x^{S_2}_{i+1} + x^{j+1}_{S_2})/\cos\theta][1-\exp(-\kappa_2\Delta x_2/\cos\theta)]^2}{1-\beta_2(\theta)} \quad \text{(A.16a)}$$

$$\Gamma_2(V_i \to P \to S_2 \to V_j) = \frac{\rho_{20}(\theta)\rho_{21}(\theta)\exp\left[\frac{-\kappa_2(x^P_i+L_2+x^{j+1}_{S_2})}{\cos\theta}\right]\left[1-\exp\left(\frac{-\kappa_2\Delta x_2}{\cos\theta}\right)\right]^2}{1-\beta_2(\theta)} \quad \text{(A.16b)}$$

and when $i > j$, we have

$$b\_\mathbf{F}^{V_j}_{V_i,1}(\theta) = \Gamma_1(V_i \to V_j) + \Gamma_1(V_i \to P \to V_j) \quad \text{(A.17)}$$

$$b\_\mathbf{F}^{V_j}_{V_i,2}(\theta) = \Gamma_2(V_i \to V_j) + \Gamma_2(V_i \to S_2 \to V_j) \quad \text{(A.18)}$$

where $\Gamma_1(V_i \to V_j)$, $\Gamma_2(V_i \to V_j)$, $\Gamma_1(V_i \to P \to V_j)$, and $\Gamma_2\ (V_i \to S_2 \to V_j)$ can be seen in Eqs. (A.7a), (A.8a), (A.15a) and (A.16a).

References

[1] C. Muresan, R. Vaillon, C. Menezo, R. Morlot, Discrete ordinates solution of coupled conductive radiative heat transfer in a two-layer slab with Fresnel interfaces subject to diffuse and obliquely collimated irradiation, J. Quant. Spectrosc. Radiative Transfer 84 (4) (2004) 551–562.
[2] S.C. Mishra, A. Lankadasu, K.N. Beronov, Application of the lattice boltzmann method for solving the energy equation of a 2-d transient conduction–radiation problem, Int. J. Heat Mass Transfer 48 (17) (2005) 3648–3659.
[3] L. David, B. Nacer, B. Pascal, J. Gerard, Transient radiative and conductive heat transfer in non-gray semitransparent two-dimensional media with mixed boundary conditions, Heat Mass Transfer 42 (4) (2006) 322–337.
[4] S.C. Mishra, H.K. Roy, Solving transient conduction and radiation heat transfer problems using the lattice boltzmann method and the finite volume method, J. Comput. Phys. 223 (1) (2007) 89–107.
[5] C.K. Krishnaprakas, N.K. Badari, P. Dutta, Combined conduction and radiation heat transfer in a gray anisotropically scattering planar medium with diffuse-specular boundaries, Int. Commun. Heat Mass Transfer 28 (1) (2001) 77–86.
[6] P. Talukdar, S.C. Mishra, Analysis of conduction–radiation problem in absorbing, emitting and anisotropically scattering media using the collapsed dimension method, Int. J. Heat Mass Transfer 45 (10) (2002) 2159–2168.
[7] J.M. Goyheneche, J.F. Sacadura, The zone method: a new explicit matrix relation to calculate the total exchange areas in anisotropically scattering medium bounded by anisotropically reflecting walls, ASME J. Heat Transfer 124 (4) (2002) 696–703.
[8] K. Daryabeigi, Heat transfer in high-temperature fibrous insulation, J. Thermophys. Heat Transfer 17 (1) (2003) 10–20.
[9] J.C. Chai, Transient radiative transfer in irregular two-dimensional geometries, J. Quant. Spectrosc. Radiative Transfer 84 (3) (2004) 281–294.
[10] M. Ben Salah, F. Askri, K. Slimi, S. Ben Nasrallah, Numerical resolution of the radiative transfer equation in a cylindrical enclosure with the finite-volume method, Int. J. Heat Mass Transfer 47 (10–11) (2004) 2501–2509.
[11] D. Byun, C. Lee, S.W. Baek, Radiative heat transfer in discretely heated irregular geometry with an absorbing, emitting, and anisotropically scattering medium using combined Monte-Carlo and finite volume method, Int. J. Heat Mass Transfer 47 (19–20) (2004) 4195–4203.
[12] D.N. Trivic, T.J. O'Brien, C.H. Amon, Modeling the radiation of anisotropically scattering media by coupling mie theory with finite volume method, Int. J. Heat Mass Transfer 47 (26) (2004) 5765–5780.
[13] D. Sarma, S.C. Mishra, P. Mahanta, Analysis of collimated radiation in participating media using the discrete transfer method, J. Quant. Spectrosc. Radiative Transfer 96 (1) (2005) 123–135.
[14] J.P. Pontaza, J.N. Reddy, Least-squares finite element formulations for one-dimensional radiative transfer, J. Quant. Spectrosc. Radiative Transfer 95 (3) (2005) 387–406.
[15] M.A. Atalay, P–N solutions of radiative heat transfer in a slab with reflective boundaries, J. Quant. Spectrosc. Radiative Transfer 101 (1) (2006) 100–108.
[16] A. Elghazaly, coupled conductive–radiative heat transfer problem for two-layer slab, J. Quant. Spectrosc. Radiative Transfer 102 (3) (2006) 482–491.
[17] H.C. Zhou, Q. Cheng, Z.F. Huang, C. He, The influence of anisotropic scattering on the radiative intensity in a gray, plane-parallel medium calculated by the DRESOR method, J. Quant. Spectrosc. Radiative Transfer 104 (1) (2007) 99–115.
[18] C.E. Siewert, A note on radiative transfer in a finite layer, J. Phys. A 40 (8) (2007) 1785–1789.
[19] F. Asllanaj, X. Brige, G. Jeandel, Transient combined radiation and conduction in a one-dimensional non-gray participating medium with anisotropic optical properties subjected to radiative flux at the boundaries, J. Quant. Spectrosc. Radiative Transfer 107 (1) (2007) 17–29.
[20] H.P. Tan, M. Lallemand, Transient radiative–conductive heat transfer in flat glasses submitted to temperature, flux and mixed boundary conditions, Int. J. Heat Mass Transfer 32 (5) (1989) 795–810.
[21] P. Sadooghi, C. Aghanajafi, Radiation effects on a ceramic layer, Radiat. Effects Defects Solids 159 (1) (2004) 61–71.
[22] P. Sadooghi, Transient coupled radiative and conductive heat transfer in a semitransparent layer of ceramic, J. Quant. Spectrosc. Radiative Transfer 92 (4) (2005) 403–416.
[23] B. Safavisohi, E. Sharbati, C. Aghanajafi, S.R.K. Firoozabadi, Effects of boundary conditions on thermal response of a cellulose acetate layer using hottel's zonal method, J. Fusion Energy 25 (3–4) (2006) 145–153.
[24] P.Y. Wang, H.E. Cheng, H.P. Tan, Transient thermal analysis of semitransparent composite layer with an opaque boundary, Int. J. Heat Mass Transfer 45 (2) (2002) 425–440.

[25] H.P. Tan, J.F. Luo, X.L. Xia, Q.Z. Yu, Transient coupled heat transfer in multilayer composite with one specular boundary coated, Int. J. Heat Mass Transfer 46 (4) (2003) 731–747.
[26] H.P. Tan, H.L. Yi, P.Y. Wang, L.M. Ruan, T.W. Tong, Ray tracing method for transient coupled heat transfer in an anisotropic scattering layer, Int. J. Heat Mass Transfer 47 (19–20) (2004) 4045–4059.
[27] R. Siegel, J.R. Howell, Thermal Radiation Heat Transfer, 4th ed., Taylor & Francis, New York, 2002. p. 85.
[28] M.T. Attia, On the exact solution of a generalized equation of radiative transfer in a two-region inhomogeneous slab, J. Quant. Spectrosc. Radiative Transfer 66 (6) (2000) 529–538.
[29] C.Y. Wu, B.T. Liou, Radiative transfer in a two-layer slab with Fresnel interfaces, J. Quant. Spectrosc. Radiative Transfer 56 (4) (1996) 573–589.
[30] H.P. Tan, J.F. Luo, L.M. Ruan, Q.Z. Yu, Transient coupled heat transfer in a multilayer composite with opaque specular surfaces and semitransparent specular interfaces, Int. J. Thermal Sci. 42 (2) (2003) 209–222.